Using Continuous GWs from Known Pulsars to Measure Gravitational Wave Speed
Project Report #2

Jake Mattinson (Caltech)
Mentors: Alan Weinstein (Caltech), Max Isi (Caltech)
LIGO SURF 2016

July 27, 2016

Abstract

Gravitational waves serve as a unique opportunity to test the strong-field highly-dynamical regime of Einstein's theory of General Relativity. In this project, we explored the possibility of detecting deviations from Einstein's predictions by examining the speed of gravitational waves. We have studied continuous gravitational waves in order to determine whether it will be possible to make a statement about the compatibility of different speeds with our observations. By considering known amplitude and phase modulation to the waveforms, we constructed a system to do a targeted search across data for signals with alternate speeds of continuous waves. Searching over actual LIGO data placed constraints on deviations from the speed of light by means of Bayesian analysis of simulated/real data corresponding to different sources.

1 Project Description

Gravitational waves (GWs) were predicted by Einstein in 1916 as a part of his development of the Theory of General Relativity (GR) and finally detected directly in September 2015 by the Laser Interferometer Gravitational wave Observatory (LIGO) [1]. Now that direct measurements of the phenomenon are possible, we can start to analyze its properties in more depth. We will attempt to directly measure the speed of GWs by analyzing months of data and searching for modulation of long-term GW signals due to Doppler shifts with periodicity of a sidereal day for different sources.

In order to measure these modifications to any accuracy, we have to take in a long period of data. We therefore will avoid sources like the black hole mergers that have already been observed with short durations, and focus on possible sources of gravitational waves which would have longer and more stable emissions. These sources, primarily rotating neutron stars (e.g. pulsars), are

expected to emit signals with very consistent frequencies and long durations but small amplitudes, generally known as continuous waves (CWs). This research will focus on known pulsars which could emit CWs, with data from the Australia Telescope National Facility pulsar catalogue (ATNF) [2]. For scale, the ATNF lists 2536 known pulsars, 291 of which are within the LIGO bandwidth (rotating at over 15 Hz).

When stationary relative to the source, one would observe the wave as a simple sinusoid, but due to the detector's motion relative to the source there is a significant frequency modulation arises due to Doppler-like effects. The mathematical framework to measure these GW signals (including heterodyning data) have been well established in the context of GWs and CWs [3, 4, 5]. However, since the first of those papers was published, GWs (but not CWs) have been observed and there have been major improvements to the sensitivity of the detectors.

2 Problem Description

In order to use the Doppler shifts of the data to measure the speed of gravitational waves, we must understand all of the different effects which shape a signal before it gets to us. We primarily consider the source's spin, the detector motion with respect to the source, and the detector orientation in this analysis.

First, we need to understand how the signal relates to the motion of the source. A basic GR result says that the frequency of the wave is double that of the source, i.e.

$$\nu_{GW} = 2\nu_{spin} \tag{1}$$

The source should emit a sinusoidal signal with some height dependent upon the physical characteristics of the source and the distance of the observer from the source

$$h(t_p) = A\sin(\theta(t_p)). \tag{2}$$

Here , t_p is the time as measured from a source at rest with respect to the source and $\theta(t_p)$ is found according to the Taylor expansion, with consideration of (1), to be

$$\theta(t_p) = \theta_0 + 4\pi\left(\nu t_p + \frac{1}{2}\dot{\nu}t_p^2 + \frac{1}{6}\ddot{\nu}t_p^3\right), \tag{3}$$

where θ_0 is a fiducial phase derived from an arbitrary starting time and a dot indicates time derivatives. Because we can observe the actual rotation of the source by using its radio emission, we know these incredibly well. For younger pulsars will often have unexplained jumps in their frequency that will quickly die down, called glitches, which can give more accurate pictures of the waveform than the above analytical model. These are seen in electromagnetic (radio) observations and can be taken as known ephemerii (from ATNF [2]). If the speed of gravitational waves is significantly different than the speed of light, c, this may render signals invisible, but these data will assume a small deviation, as predicted in most theories [3].

Next, we need to understand the sensitivity of the detector. Unlike a telescope, which is movable and limited in its observation region, LIGO is an observatory that is sensitive to signals from every direction and cannot be aimed. This means that the detectors should be modeled like antennas which have sensitivity based on the polarization of the signal, the location of the source, and the orientation of the detector. We can define a set of vectors which define the detector: $\mathbf{d}_z$ points from the center of the Earth to the detector, $\mathbf{d}_x$ and $\mathbf{d}_y$ are unit vectors that point along its arms. We then define the orientation of the pulsar with unit vectors: $\mathbf{w}_z$ is the vector from the source toward the detector, $\mathbf{w}_x$ points along the local East orientation for the pulsar, and $\mathbf{w}_y$ is perpendicular to both of those at a local North. This can be seen below:

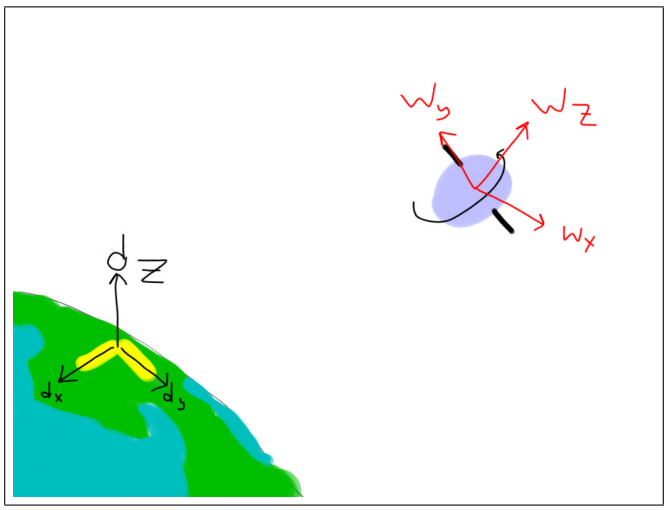

Figure 1: TEMPORARY IMAGE This image shows the definitions of the vectors which define the source-detector system.

GR predicts that CWs would have two polarizations: plus (+) and cross (×). Waves with these polarizations stretch spacetime perpendicular to their direction of propagation: shrinking it in one direction and expanding it in the other. These two polarizations are almost the same, excepting a 45° rotation from one to the other (hence their names). The detector sensitivity to each will be different, based on the geometry of the setup. Using the above definitions, we can derive the following sensitivities, or antenna patterns (APs):

$$F_+ = \frac{1}{2}[(\mathbf{w}_x \cdot \mathbf{d}_x)^2 - (\mathbf{w}_x \cdot \mathbf{d}_y)^2 - (\mathbf{w}_y \cdot \mathbf{d}_x)^2 + (\mathbf{w}_y \cdot \mathbf{d}_y)^2], \tag{4}$$

$$F_\times = (\mathbf{w}_x \cdot \mathbf{d}_x)(\mathbf{w}_y \cdot \mathbf{d}_x) - (\mathbf{w}_x \cdot \mathbf{d}_y)(\mathbf{w}_y \cdot \mathbf{d}_y). \tag{5}$$

The changing nature of the observatory position implies that the antenna pattern varies across a sidereal day and affects the amplitude of the signal, leading to amplitude modulation (AM). These equations, if expanded analytically,

can be written as trigonometric functions in terms of twice the azimuthal angles of the source, i.e. we will expect a period of half a day as well as a full day (diurnal) cycle.

Now, we can actually discuss the Doppler and relativistic delays. This can be expressed as the sum:

$$t_b = t + \Delta_E + \Delta_S + \Delta_R, \tag{6}$$

where t_b is the time measured from the Solar System Barycenter (SSB), t is the time measured on Earth, Δ_E is the Einstein delay due to Special Relativity, Δ_S is the Shapiro delay from GR, and Δ_R is the Rømer delay due to changing distances within orbits/rotations. Δ_E is practically constant in relevant timescales, so it is ignorable. Δ_S is of order $10^{-7}s$ [6], far below our timescales, making it ignorable. We only have to calculate the Rømer delay. This is given by the formula:

$$\Delta_R = \frac{\vec{r} \cdot \hat{n}}{c_g} \tag{7}$$

where $\vec{r}$ points from the SSB to the detector, $\hat{n}$ is the unit vector pointing from the source to the SSB, and c_g is the speed of the gravitational wave. We will assume $\hat{n}$ is constant with direction $\hat{n}_0$, as the source is effectively at rest relative the SSB. We know $\vec{r}$ has two components: $\vec{r} = \vec{R} + \vec{s}$ where $\vec{R}$ points from the SSB to the center of Earth and $\vec{s}$ points from Earth to the detector. $\vec{R}$ oscillates over a year while $\vec{s}$ has periodicity of a sidereal day. For most purposes, we will mostly ignore the influence of $\frac{|d\vec{R}|}{dt}$ as $\left|\frac{d\vec{s}}{dt}\right| \approx 1.6 \times 10^{-2} \left|\frac{d\vec{R}}{dt}\right|$ (and it should be mentioned that $\left|\frac{d\vec{s}}{dt}\right| \approx 1.55 \times 10^{-6}\, c$).

The Rømer delay is where the speed of the gravitational wave comes into play as it induces a frequency modulation (FM). A very small speed would yield a very significant Rømer delay. Currently, the LIGO Algorithm Library (`LALSuite`) assumes that $c_g = c$.

We now know how to model a wave with all of the applicable dynamics. Now that the wave has traveled to the detector, the raw data goes through a long process in order to search for a signal. For continuous waves with a known source, the procedure is the following:

1. **Raw data is collected**

   This step is beyond the scope of this project, but it suffices to mention that the data is dominated by noise and is sampled at $f_s = 16,384\,\text{Hz}$.

2. **Heterodyne**

   We want to see the amplitude modulation of the signal, so we want to use heterodyning. First, we decompose the signal $h(t)$ into:

   $$h(t) = \Lambda(t)e^{i\theta(t)} + \Lambda^*(t)e^{-i\theta(t)} \tag{8}$$

   for some $\Lambda(t)$ and $\theta(t)$. As others have shown [8][7], we know the following:

   $$h(t) = h_+(t)\cos\,\theta(t) + h_\times(t)\sin\,\theta(t) \tag{9}$$

this allows us to compute calculate $\Lambda(t)$ with some magnitude $h_0 = \sqrt{h_+^2 + h_\times^2}$:

$$\Lambda(t) = h_0 \left(\frac{1 + \cos^2 \iota}{4} F_+(t) + \frac{i \cos \iota}{2} F_\times(t) \right) \tag{10}$$

where ι is the relative inclination angle of the source relative the Earth. We also know that $\theta(t)$ is derived from the source rotation as shown in eq. 3, so we can actually make this information useful.

However, we do not want to look for the high frequency from the pulsar (via (3)) as their data can be boiled into just the slower AM and FM of the antenna pattern implied by eqs (4) & (5). Heterodyning the process which allows us to achieve that. We can take the entire strain and multiply it by $e^{-i\theta(t)}$ to get

$$h_{\text{het}}(t) = e^{-i\theta(t)} \cdot h(t) = \Lambda(t) + \Lambda^*(t) e^{-2\theta(t)} \tag{11}$$

which yields a very low frequency and a very high frequency one. For the Crab Pulsar, this would have frequencies of about 0.00002 Hz (an inverse sidereal day) and 120 Hz (as the Crab rotates at about 60 Hz), respectively. It may be important to note here that even though the signal was purely real, we now are working in the complex domain.

It should also be mentioned that since the Rømer delay is implemented in this step, this pre-processing may reveal the difference in speed as current implementations assume $c_g = c$.

If that assumption is not true, however, eqn. (11) does not hold. Using eq. (8), we see that the waveform is dependent upon the speed of CWs. Therefore we can define $\theta(t; v)$ for some perceived speed of gravitational wave v. Let $\delta\theta(t) = \theta(t; c_g) - \theta(t; c)$. This means that in the heterodyne we may not cancel out the modulation completely and could instead be left with

$$h_{\text{het}}(t) = \Lambda(t) e^{i\delta\theta(t)} + \Lambda^*(t) e^{-i(\theta(t;c_g)+\theta(t;c))} \tag{12}$$

3. **Filters (e.g. Butterworth) applied**

   This process is not yet applicable to this research, but this low pass filter (LPF) removes some noise and much of the high frequency features.

4. **Downsample**

   Downsampling serves as another LPF, where higher frequency signals are completely lost, so the second term in eq.(8) is removed. As the name implies, downsampling involves reducing the number of points in the data being analyzed from the points present. To do this for CWs, LIGO takes one minute sized chunks and takes their average. This means that from

the heterodyned signal $s[i]$, sampled at about a high frequency, the new signal will have terms

$$B_k = \frac{1}{M} \sum_{i=1}^{M} h_{het}(t_i) \tag{13}$$

where M is the total number of samples in a minute.[7] For actual LIGO data, this takes the sampling rate from 16384 Hz to $\frac{1}{60}$ Hz.

Downsampling and low pass filtering removes the high frequency signal from (12). This yields the following measurement of speed:

$$\frac{h_{\text{ds, het}}(t)}{\Lambda(t)} = e^{i\delta\theta(t)}. \tag{14}$$

Seeing this modulation amid the noise is now equivalent to finding the speed of gravitational waves.

3 Progress

I created "toy models" for all of the above, using generic or standard assumptions. This was my primary focus for my first six weeks.

In order to visualize the Rømer delay, one can plot it and find something like the following:

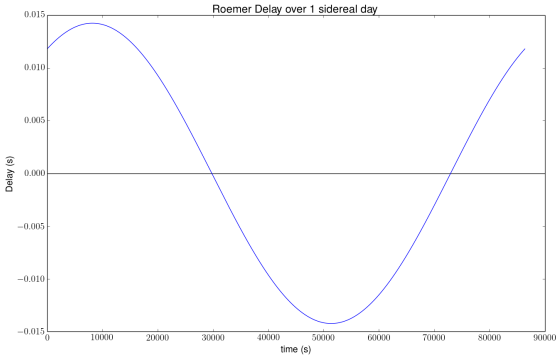

Figure 2: The Rømer delay over a sidereal day approximately makes a sinusoid, with smaller effect across a year.

It is significant that this is a sinusoid and that this has a non-negligible magnitude. Once we understand the delay, we want to plot the antenna patterns. We set $\mathbf{d}_x$ and $\mathbf{d}_y$ to be the x and y axes, with source position being arbitrary. Below are three pictures for the simplest case, with source aligned with the detector[8]:

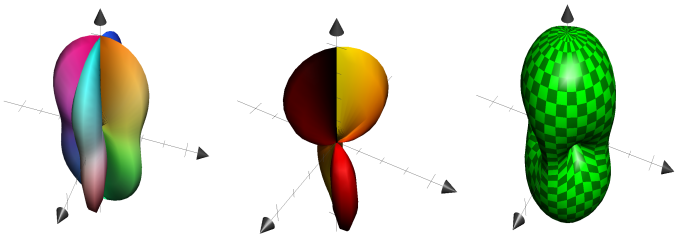

(a) Plus (F_+) (b) Cross ($F_\times$) (c) $\sqrt{F_+^2 + F_\times^2}$

Figure 3: Antenna patterns for the two GR polarizations

The distance from the center origin at any angle indicates the sensitivity of the detector to that polarization at that angular position relative to the detector arms (the x and y axes). It should be noted that the magnitude of subfigure 3.c is invariant under changes of the relative rotation angle, as plus and cross polarizations become identical and switch functions under certain rotations. These figures, while interesting, are not particularly useful in and of themselves. The sensitivity changes over a day because of the Earth's rotation. This is dependent heavily on the positions of the observatory and the source (via (4) and (5)). Implementing these for the Crab Pulsar and both observatories then yields the following plots for the AM $\Lambda(t)$:

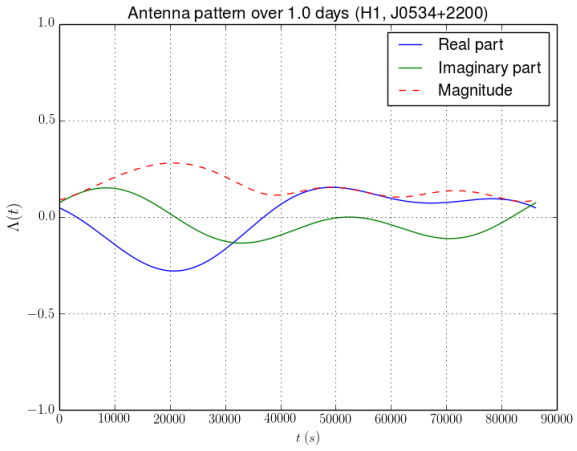

(a)

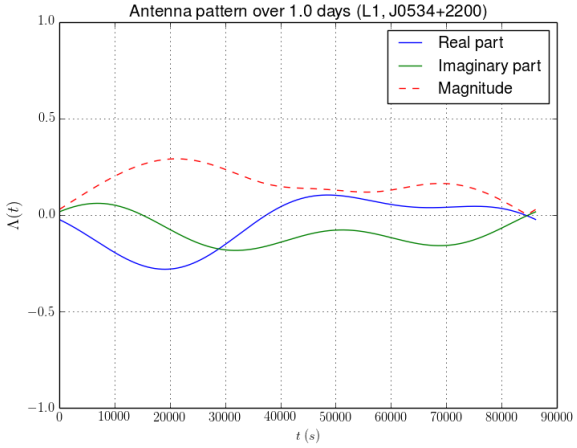

(b)

Figure 4: Overall sensitivity to Crab pulsar over a day at the (a) Hanford and (b) Livingston Observatories

In order to check that this has the two frequencies we expect, we Fourier transform it. If we look closely, we can see the two frequencies we anticipate, as shown below.

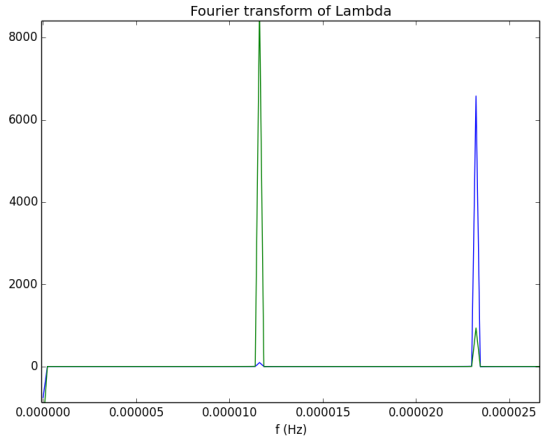

Figure 5: Fourier transform of the data, zooming in on the barely noticeable bumps near 0; blue is real, green is imaginary. The three visible bumps represent an inherent term at frequency 0, the diurnal cycle at about 1/86164 Hz, and the twice diurnal cycle at about 1/43082 Hz. These plots agree with the official LIGO plots made in `LALSuite`.

It is at this point necessary to implement the mathematical concepts established using eqs. 8 - 13. To show this in practice, we generated a day of a fake signal with amplitude modulation $\Lambda(t) = 5 + \cos(\frac{2\pi\, t}{86164s})$ and fast sinusoid (signal) of $h(t) = \Lambda(t) \cdot \sin(2\pi \cdot 0.01\text{Hz} \cdot t)$. For this research, the frequency (0.01 Hz) would be much higher (e.g. 60 Hz), but for visualization it is low frequency. The data are shown below:

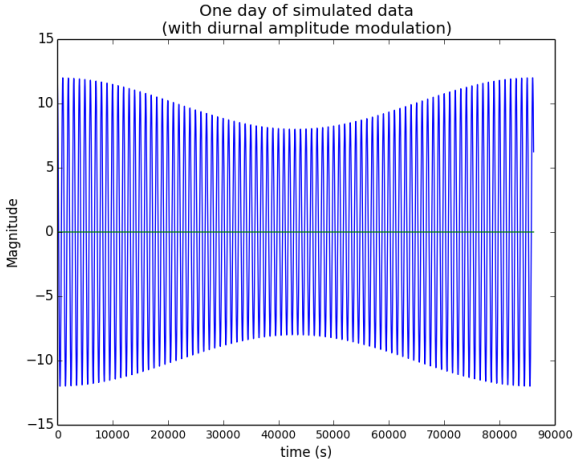

Figure 6: The simulated signal for a some time. Note the amplitude modulation.

The amplitude follows a sinusoidal progression at about 3 times the length of this frame. Now, since we know the $\theta(t)$ that we would plug into eqn. (11), we can heterodyne to get the following plot:

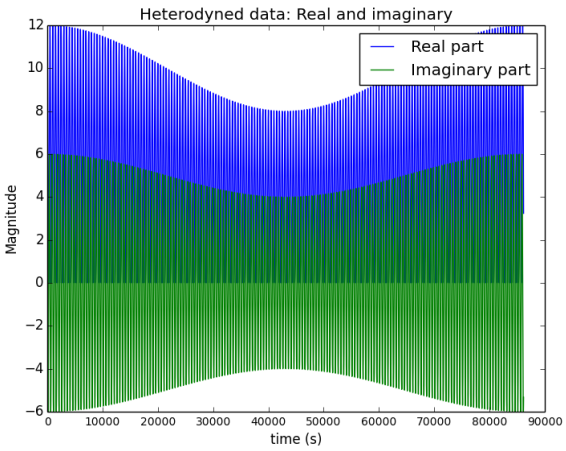

Figure 7: Heterodyne of the above data with known frequency evolution.

We can see the faster wave as well as the still slow wave in the amplitude modulation which equation (11) predicts.

Next, we take that data and downsample significantly (here, downsampling was by a factor of a few thousand), taking an average over every segment. This eliminates the high frequency data and leaves a signal at half of the amplitude of the waves.

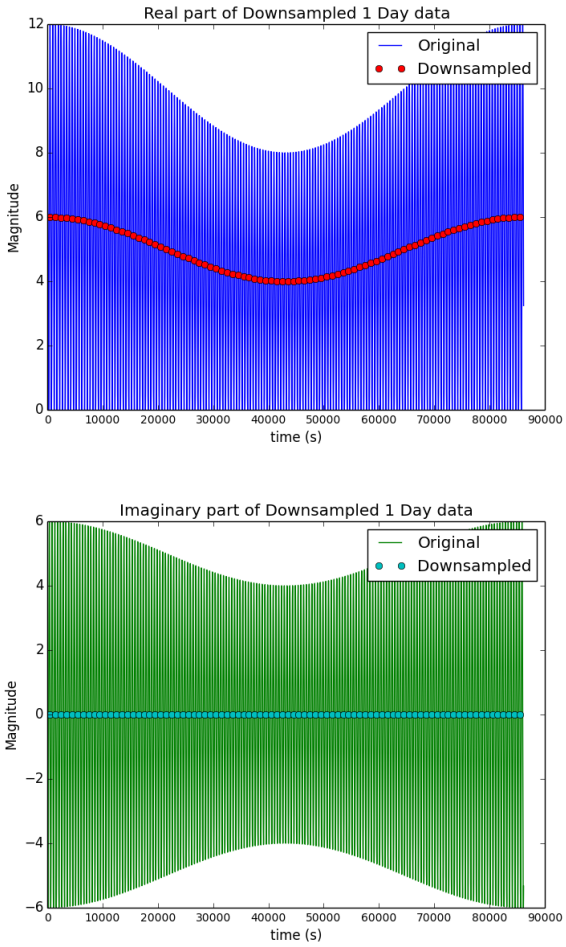

Figure 8: Real and imaginary parts of the downsampling from the heterodyned data. Note how the real part represents half of the amplitude of the final wave and the imaginary part goes to zero; this reflects the original data's purely real component.

In the above implementation there were some simplifications. The sinusoids were all constant in their frequency (i.e. $d^2\theta/dt^2 = 0$), ignoring both $\dot{\nu}$ and $\ddot{\nu}$ terms. In reality, this is a close approximation, but not exact. We know that the source has a rotational speed of $\nu(t)$ which varies significantly. With older pulsars, this is a pretty smooth rate, but for younger pulsars, unexpected errors happen at a significant rate. These glitches are seen in the EM spectrum, so if $c_g \approx c$, these should align pretty well in time and allow us to use astronomical observations during the time of observation in order to model the frequency of the expected wave. If $c_g << c$, this phase evolution may hurt the search, but

that case is not expected [9]. Furthermore, this model ignores the Rømer delay in order to simplify the visualization. Therefore the FM has zero impact here.

4 Goals

I hope to use the MCMC package `emcee` in order to create probability distribution functions (PDFs) across different possible values of c_g for different sources.

After that, I will focus on moving away from the toy models that I am currently creating, implementing with actual LIGO data. Once we've analyzed data from O1, then we will hope to see the modulation in any way, at least giving a bound on the difference between the two speeds.

5 Challenges

Most of the challenges have been in simply doing the science and being able to be enthused about a tough problem when I'm tired.

6 Resources

I will eventually start to use one of LIGO's computer clusters to analyze data if my laptop stops being sufficiently fast, but otherwise, my mentors have been helpful enough for me to make it through.

References

[1] B.P. Abbott et al. Observation of gravitational waves from a binary black hole merger. *Physics Review Letter*, 116, 2016.

[2] A. Teoh & M. Hobbs AJ R.N. Manchester, G.B. Hobbs. Web, 1993-2006 (2005).

[3] Max Isi. Detecting deviations from general relativity using continuous gravitational waves. *LIGO*, 2013.

[4] Carver Mead Maximiliano Isi, Alan J. Weinstein and Matthew Pitkin. Detecting beyond-einstein polarizations of countinuous gravitational waves. *LIGO*, 2015.

[5] Atsushi Nishizawa et al. Probing nontensorial polarizations of stochastic gravitational-wave backgrounds with ground-based laser interferometers. *Physical Review Letters*, 79, 2009.

[6] Edwin F. Taylor and Edmund Bertschinger. *Exploring Black Holes: Introduction to General Relativity 2nd ed.* Addison Wesley Longman, San Francisco, 2000.

[7] Matthew Pitkin. *Prospects of observing continuous gravitational waves from known pulsars*. PhD thesis, California Institute of Technology, 2011.

[8] Max Isi et. al. Detecting beyond-einstein polarizations of continuous gravitational waves. *LIGO*, April 2015.

[9] Matthew Pitkin Garth S. Davies and Graham Woan. A targeted spectral interpolation algorithm for the detection of continuous gravitational waves. 2016.